

Phase-flip transition in nonlinear oscillators coupled by dynamic environment

Amit Sharma, Manish Dev Shrimali, and Syamal Kumar Dana

Citation: *Chaos: An Interdisciplinary Journal of Nonlinear Science* **22**, 023147 (2012); doi: 10.1063/1.4729459

View online: <http://dx.doi.org/10.1063/1.4729459>

View Table of Contents: <http://scitation.aip.org/content/aip/journal/chaos/22/2?ver=pdfcov>

Published by the [AIP Publishing](#)

Articles you may be interested in

[Phase and amplitude dynamics in large systems of coupled oscillators: Growth heterogeneity, nonlinear frequency shifts, and cluster states](#)

Chaos **23**, 033116 (2013); 10.1063/1.4816361

[Universal occurrence of the phase-flip bifurcation in time-delay coupled systems](#)

Chaos **18**, 023111 (2008); 10.1063/1.2905146

[Delay time modulation induced oscillating synchronization and intermittent anticipatory/lag and complete synchronizations in time-delay nonlinear dynamical systems](#)

Chaos **17**, 013112 (2007); 10.1063/1.2437651

[Experimental evidence of anomalous phase synchronization in two diffusively coupled Chua oscillators](#)

Chaos **16**, 023111 (2006); 10.1063/1.2197168

[Experimental investigation of partial synchronization in coupled chaotic oscillators](#)

Chaos **13**, 185 (2003); 10.1063/1.1505811



Phase-flip transition in nonlinear oscillators coupled by dynamic environment

Amit Sharma,¹ Manish Dev Shrimali,² and Syamal Kumar Dana³

¹The LNM Institute of Information Technology, Jaipur 302031, India

²Indian Institute of Technology Rajasthan, Jodhpur 342011, India

³Central Instrumentation, CSIR-Indian Institute of Chemical Biology, Kolkata 700032, India

(Received 4 October 2011; accepted 31 May 2012; published online 18 June 2012)

We study the dynamics of nonlinear oscillators indirectly coupled through a dynamical environment or a common medium. We observed that this form of indirect coupling leads to synchronization and phase-flip transition in periodic as well as chaotic regime of oscillators. The phase-flip transition from in- to anti-phase synchronization or vice-versa is analyzed in the parameter plane with examples of *Landau-Stuart* and *Rössler* oscillators. The dynamical transitions are characterized using various indices such as average phase difference, frequency, and Lyapunov exponents. Experimental evidence of the phase-flip transition is shown using an electronic version of the van der Pol oscillators. © 2012 American Institute of Physics. [<http://dx.doi.org/10.1063/1.4729459>]

Many synchronization phenomena, in nature, occur by indirect interaction between individual oscillators via a common medium or common dynamic environment. Examples in physical, engineering, and even biological systems are abundant. Recently, another type of indirect interaction is found in synthetic genetic oscillators that are able to induce different synchronization regimes, in-phase, anti-phase, homogeneous or inhomogeneous steady states and even coexisting synchronization states. There the individual genetic oscillators interact with each other via small molecules released by each of them in a common medium. The small molecules, in turn, interact with each other directly and eventually induce a quorum sensing type of coupling between the genetic oscillators. One natural question arises whether the coherent behaviors induced by such coupling is system specific or generic in nature. To explore this, we applied this quorum sensing type indirect coupling to benchmark dynamical systems, *Landau-Stuart* (LS) model and *Rössler* oscillators, when we observed both the in-phase and anti-phase states but, in addition, we observed a typical phase-flip transition. In phase-flip transition, synchronized oscillators switch from a state of in-phase to anti-phase or vice-versa. The phase difference between the oscillators undergoes a jump of π as a function of a control parameter and it is accompanied by discontinuous changes in the common frequency of the synchronized oscillators. In most of the cases, the control parameter is considered as a delay in the coupling function. In some other cases, it is observed in dynamical systems in presence of relaying interactions.¹ Here, we showed that the phase-flip (PF) transition can be observed under indirect dynamical coupling in absence of any delay in the coupling. We provide experimental evidence of the phase-flip transition under indirect coupling in electronic circuits of van der Pol oscillators.

I. INTRODUCTION

In the last two decades, synchronization phenomenon has been extensively studied in interacting dynamical systems due

to its great potential in physical, engineering, biological, and social systems.² Various synchronization regimes including, complete synchronization,³ in-phase,⁴ anti-phase,^{5,6} lag synchronization,⁷ generalized synchronization,⁸ intermittent lag synchronization,⁹ and mixed-synchronization¹⁰ have been identified in nonlinear oscillators. These synchronization states can be realized through interaction of oscillators via diffusive,¹¹ conjugate,¹² delay,¹³ and nonlinear coupling.¹⁴ A few important consequences of the coupling in nonlinear dynamical systems such as *PF* transition¹⁵ and amplitude death (*AD*)^{16,17} were reported in the recent past. In a *PF* transition, relative phase of the oscillators jumps from zero to π or vice versa as a coupling parameter is varied. The *PF* transition has broad relevance to natural systems especially under time delay coupling.¹⁵ This phase-flip phenomenon has so far been explored in semiconductor lasers,¹⁸ electrochemical cells,¹⁹ and delay coupled neuron models, ecological models, and electronic circuits²⁰ in the periodic as well as chaotic regime. Recently, the phase-flip transitions are also observed in a network of coupled bursting neurons.²¹ The *PF* transition was usually seen as an attribute of a delay present in the coupling until a report is published very recently on relay coupled *Rössler* oscillator where the *PF* transition is first reported in absence of coupling delay.¹

In contrast to the conventional direct coupling as mentioned above, recently some indirect form of coupling was used in the context of studies on collective behaviors of real world systems. As examples, cellular populations communicating via small molecules that freely diffuse into a common medium,^{22,23} pendulum clocks mounted on the same wooden beam,²⁴ chemical oscillators interacting via a common solution,²⁵ global oscillation of neuro-transmitter in a population of circadian oscillator,²⁶ ensemble of cold atom interacting with electromagnetic field,²⁷ longitudinal modes of lasers connected through saturation of common amplifying medium,²⁸ and indirectly coupled periodic as well as chaotic systems.²⁹ Dynamical systems indirectly coupled through a common dynamical medium or environment show a variety of synchronized behaviors, including in-phase and anti-phase.

In the present work, we investigate the effect of indirect coupling on nonlinear oscillators via a dynamic environment mostly found in genetic oscillators.^{22,23} Interestingly, we find that this type of indirect interaction in dynamical systems not only leads to a variety of synchronization regimes but also shows a *PF* transition in absence of any coupling delay. We report, in detail, examples of two model systems: LS and *Rössler* oscillators. A *PF* transition is characterized by computing the average phase difference, frequency and Lyapunov exponents. Further, we constructed electronic circuits of two van der Pol oscillators to make an experimental demonstration of the *PF* transition under the interaction of dynamic environment. These results indicate an emergence of an inherent delay in the exchange of information between the two oscillators coupled indirectly through local dynamic environment causing the *PF* transition.

This paper is organized as follows. In the next section, Sec. II, a general description of the *PF* transition via indirect coupling is given. The *PF* transition from in-phase to anti-phase synchronization or vice versa with inherent bistability in *PF* transition is elaborated using LS and *Rössler* oscillators in Sec. III. The experimental setup and demonstration of *PF* transition in coupled van der Pol oscillators is given in Sec. IV followed by Conclusions.

II. ENVIRONMENTAL COUPLING

Consider two nonlinear oscillators coupled indirectly through dynamic agents in a local medium or environment²³

$$\dot{X}_i = F(X_i) + \kappa S_i, \quad \dot{S}_i = G(S_i, S_j, X_i), \quad (1)$$

where for $i, j = 1, 2$, X_i is the state variable of the i th nonlinear oscillator and S_i is its agent interacting with the other agents S_j in a common environment, having dimensions m_X and m_S , respectively. $F(\cdot)$ and $G(\cdot)$ specify the evolution equations of the i th oscillator and its i th agent, respectively. The i th dynamical system is directly interacting with its local agent S_i with a strength κ and all these agents S_i interact directly with each other in a common dynamic environment or medium (Fig. 1). In the case of biological cells, X_i would be a vector whose components are the concentrations of various biochemical species in cell i , and S_i a vector of concentrations of various biochemical species in the exterior of the cells. This has analogy with small molecules released by cells into a common medium,²³ where all the small molecules develop a global interaction and as a result

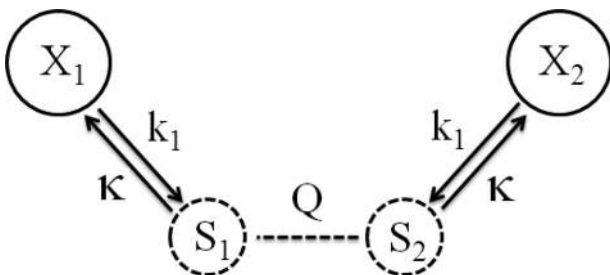


FIG. 1. Coupling scheme of dynamical systems coupled through dynamic environment.

the cells emerge into different collective regimes via indirect interaction.

The dynamics of each agent S_i under interaction with other agents is given by,

$$\dot{S}_i = -k_0 S_i + k_1 X_i - \eta(S_i - Q\langle S \rangle). \quad (2)$$

The intrinsic dynamics of S_i is decaying with a rate constant k_0 but it is enhanced by one of the variables of the i th dynamical system with a growth rate k_1 . S_i is also influenced by the interaction with other agents in the common medium or dynamical environment.²³ η is a diffusion constant and $\langle S \rangle$ is a mean field average defined by $(S_1 + S_2)/2$ here for two oscillators. Q is the strength of the mean field interaction of all the agents influencing the collective dynamics of the oscillators. In this coupling scheme, interaction between the dynamical systems is maintained through its agents which, in turn, interact globally with each other in the common dynamic environment. The dynamic environment thus supports an indirect process of information exchange for synchronization and eventually a phase-flip transition in the dynamical systems which we are mainly interested to explore here. We define this indirect form of interactive process as *environmental coupling* in the rest of the text.

III. PHASE FLIP TRANSITION: NUMERICAL RESULTS

Transition from in-phase to anti-phase synchronization or vice-versa is studied numerically using average phase difference between the coupled systems and their common frequency. We define the instantaneous phase ϕ_i of the i th oscillator by

$$\phi_i(t) \cong \text{atan} \left(\frac{y_i(t) - y_i^*}{x_i(t) - x_i^*} \right), \quad (3)$$

where $x_i(t), y_i(t)$ are the state variables and x_i^*, y_i^* are the fixed point of the oscillators. The average phase difference $\Delta\phi_{ij}$ between i and j -th oscillators is

$$\Delta\phi_{ij} = \langle |\phi_i - \phi_j| \rangle \quad i, j = 1, 2, \dots, N, \quad (4)$$

where $\langle \cdot \rangle$ denotes an average over time.

The common frequency of a coupled dynamical system is estimated using summation of average rate of change in instantaneous phase

$$\Omega = \frac{1}{N} \sum_{i=1}^N \Omega_i = \frac{1}{N} \sum_{i=1}^N \left\langle \frac{d\phi_i(t)}{dt} \right\rangle. \quad (5)$$

A. Landau-Stuart oscillators

We first consider the *Landau-Stuart* oscillators coupled through dynamic environment

$$\begin{aligned} \dot{x}_i &= (1 - (x_i^2 + y_i^2))x_i - \omega_i y_i, \\ \dot{y}_i &= (1 - (x_i^2 + y_i^2))y_i + \omega_i x_i + \kappa S_i, \\ \dot{S}_i &= -k_0 S_i + k_1 y_i - \eta \left(S_i - \frac{Q}{2} \sum_{j=1}^2 S_j \right). \end{aligned} \quad (6)$$

where $i, j = 1, 2$. In uncoupled state ($\kappa = 0, k_1 = 0$ and $\eta = 0$), each oscillator has a fixed point $(x_i^*, y_i^*) = (0, 0)$ which is unstable with eigenvalue $1 + i\omega_i$. In coupled state, we choose the parameter values as $\omega_1 = \omega_2 = 9.0, k_0 = 1, \eta = 10$ when we explore the regime of *PF* transition in κ - Q and k_1 - Q parameter space. To predict the *PF* transition in coupled *LS* limit-cycle oscillator as described by Eqs. (6), we derive the Jacobian matrix of the coupled *LS* oscillator at origin,

$$\begin{pmatrix} p_1 & -\omega & 0 & 0 & 0 & 0 \\ \omega & p_1 & \kappa & 0 & 0 & 0 \\ 0 & k_1 & \mu_1 & 0 & 0 & \mu_2 \\ 0 & 0 & 0 & p_2 & -\omega & 0 \\ 0 & 0 & 0 & \omega & p_2 & \kappa \\ 0 & 0 & \mu_2 & 0 & k_1 & \mu_1 \end{pmatrix}, \quad (7)$$

where $\mu_1 = -k_0 - \eta + \eta Q/2, \mu_2 = \eta Q/2$ and $p_i = 1 - \zeta$. We approximate that the time average values of the $(x_i^2 + y_i^2)$ are same for both the oscillators and replace it by an effective constant ζ_i . The angular frequency of the i th system is ω_i . For simplicity, we consider identical oscillators $\omega_1 = \omega_2 = \omega$. We assume that the origin is one of the fixed points of the coupled limit-cycle oscillator under the influence of dynamical environment, i.e., $(x_i^*, y_i^*, s_i^*) = (0, 0, 0)$, which is unstable for the given parameters. The characteristic equation of the Jacobian matrix is

$$(a_1 - (\mu_1 + \mu_2)a_2)(a_1 + (\mu_1 - \mu_2)a_2) = 0, \quad (8)$$

where $a_1 = (\lambda^3 - 2p\lambda^2 + (p^2 + \omega^2 - k_1\kappa)\lambda + pk_1\kappa), a_2 = ((p^2 - \lambda^2) + \omega^2)$. Since this equation is difficult to solve analytically, we compute the eigenvalues of characteristic Eq. (8) numerically. We calculated the eigenvalues related to the unstable fixed point and observed that the phase-flip transition in coupled system occurs when the real part of complex eigenvalue (positive) cross each other (i.e., $Re(\lambda_k) = Re(\lambda_l), k, l = 1, 2, \dots, n$) at the critical coupling $Q = Q_c$, as reported in Ref. 30. Moreover, we observed that the *PF* transition boundary separates the in-phase and the anti-phase region in a $\kappa - Q$ and $k_1 - Q$ parameter plane (Fig. 2). For

instance on the left side of the boundary $Re(\lambda_{3,4}) > Re(\lambda_{5,6})$ where an in-phase region exists while on the right side, $Re(\lambda_{3,4}) < Re(\lambda_{5,6})$, the anti-phase region exists. Numerical results in dotted line are in close agreement with the analytical results in solid line of the *PF* transition. As κ (or k_1) decreases, the feedback from the environment s to variable y (or feedback from oscillatory system to environment) is reduced. However, sufficient interaction between the oscillatory systems and environment is essential for the phase-flip tendency. This leads to the deviations for small values of κ (or k_1). For large values of k_1 , the feedback from the oscillatory system to environment is too strong that again leads to the deviations while strong feedback from environment does not affect the dynamical behaviour of the oscillatory system of large amplitude.

The Lyapunov exponents of the coupled *LS* oscillators are plotted with coupling parameter Q at $k_1 = 0.5$ and $\kappa = 25$ as shown in Fig. 3(a). The largest Lyapunov exponent remains at zero with the increase of Q . When second Lyapunov exponent starts decreasing below zero, it indicates² onset of phase synchronization. The in-phase synchrony of the coupled oscillators is shown in Fig. 3(c). With increase of Q , the second Lyapunov exponent reaches to zero once again and then makes a discontinuous jump to a negative value at $Q_c = 0.47$ that clearly indicates the *PF* transition in the coupled *LS* oscillators. This is accompanied by a sudden increase of the common oscillation frequency which jumps from ~ 8.52 to ~ 8.73 as shown in Fig. 3(b). Time series of both the oscillators show in-phase synchronization when $Q < Q_c$ (Fig. 3(c)) while out-of-phase when $Q > Q_c$ (Fig. 3(d)). Similarly, Lyapunov exponents and common frequency of the coupled Landau Stuart oscillators are investigated by varying κ at a fixed $Q = 0.45$ (Figs. 3(e) and 3(f)). Once again, we observed a *PF* transition as revealed by discontinuous change in the Lyapunov exponents and the common frequency. However, the frequency of the coupled oscillators jumps to a lower value at the transition point $\kappa_c = 20.3$ since an inverse *PF* transition from anti-phase to in-phase state occurs. The pair of time series of the coupled Landau Stuart oscillators before ($\kappa = 18$) and after ($\kappa = 22$) the transition is shown in Figs. 3(g) and 3(h).

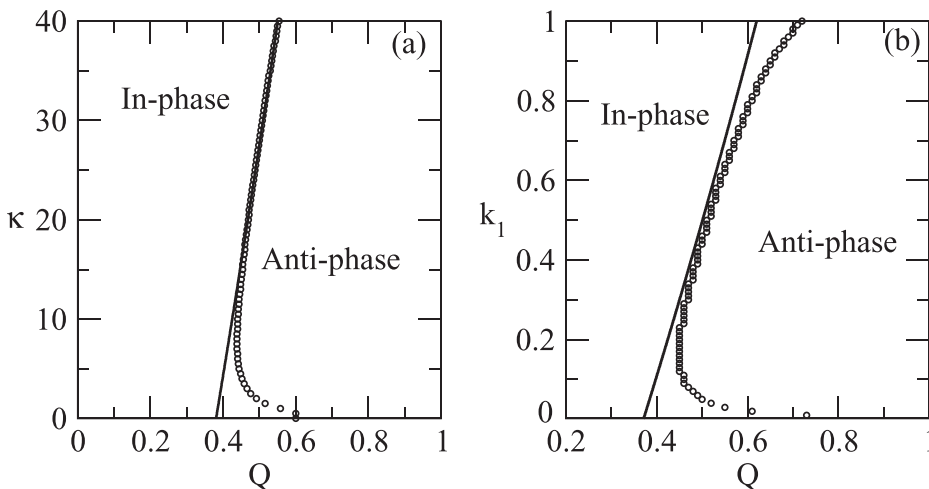


FIG. 2. Transition from in-phase to anti-phase state is shown in parameter plane (a) $\kappa - Q$ at $k_1 = 0.5$ and (b) $k_1 - Q$ at $\kappa = 30$ for Landau-Stuart oscillator coupled through dynamical environment. The dotted line shows numerically simulated phase-flip transition from in- to anti-phase state. Solid curve is a fitting of the phase-flip criterion ($Re(\lambda_{3,4}) = Re(\lambda_{5,6})$) obtained from the real part of the eigenvalues with effective constant $\zeta = 0.96$.

Bistability is an important behavior observed under environment coupling²³ and in relay coupled oscillators.¹ We observed coexisting stable states near the transition in LS oscillators coupled through dynamic environment, in the sense, that not all sets of initial conditions show phase-flip transition at a same Q value. Some sets of initial conditions show anti-phase synchronization while others show in-phase synchronization.¹ To illustrate this behavior, we plot the phase difference $\Delta\phi_{12}$ average over time as a function of Q taking 100 different sets of initial conditions which confirmed that the transition does not occur at one critical parameter Q_c and stretches over a Q range ranging from 0.45 to 0.52 (see Fig. 4(a)).

B. Rössler oscillators

As a second example, we consider chaotic Rössler oscillators³¹ interacting through dynamic environment,

$$\begin{aligned} \dot{x}_i &= -w_i y_i - z_i, \\ \dot{y}_i &= w_i x_i + a y_i, \\ \dot{z}_i &= b + z_i(x_i - c) + \kappa s_i, \\ \dot{s}_i &= -k_0 s_i + k_1 z_i - \eta \left(s_i - \frac{Q}{2} \sum_{j=1}^2 s_j \right), \end{aligned} \tag{9}$$

where $a=0.165$, $b=0.4$, $c=8.5$, $\omega_i=0.97$ (internal frequency), $k_0=1$, $\eta=2$, and $Q \in [0, 1]$.

The relative phase difference of the coupled Rössler oscillators is studied in the $\kappa - Q$ and $k_1 - Q$ parameter plane (Shown in Figs. 5(a) and 5(b)). We find a type of coexisting synchronization (in-phase and anti-phase) with unsynchronized state for $\kappa \simeq 5$ and $k_1 \simeq 0.2$, respectively. With further increase of κ or k_1 , the coupled Rössler oscillators start synchronizing in anti-phase state and in-phase state for lower and higher values of Q , respectively, as shown in Fig. 5.

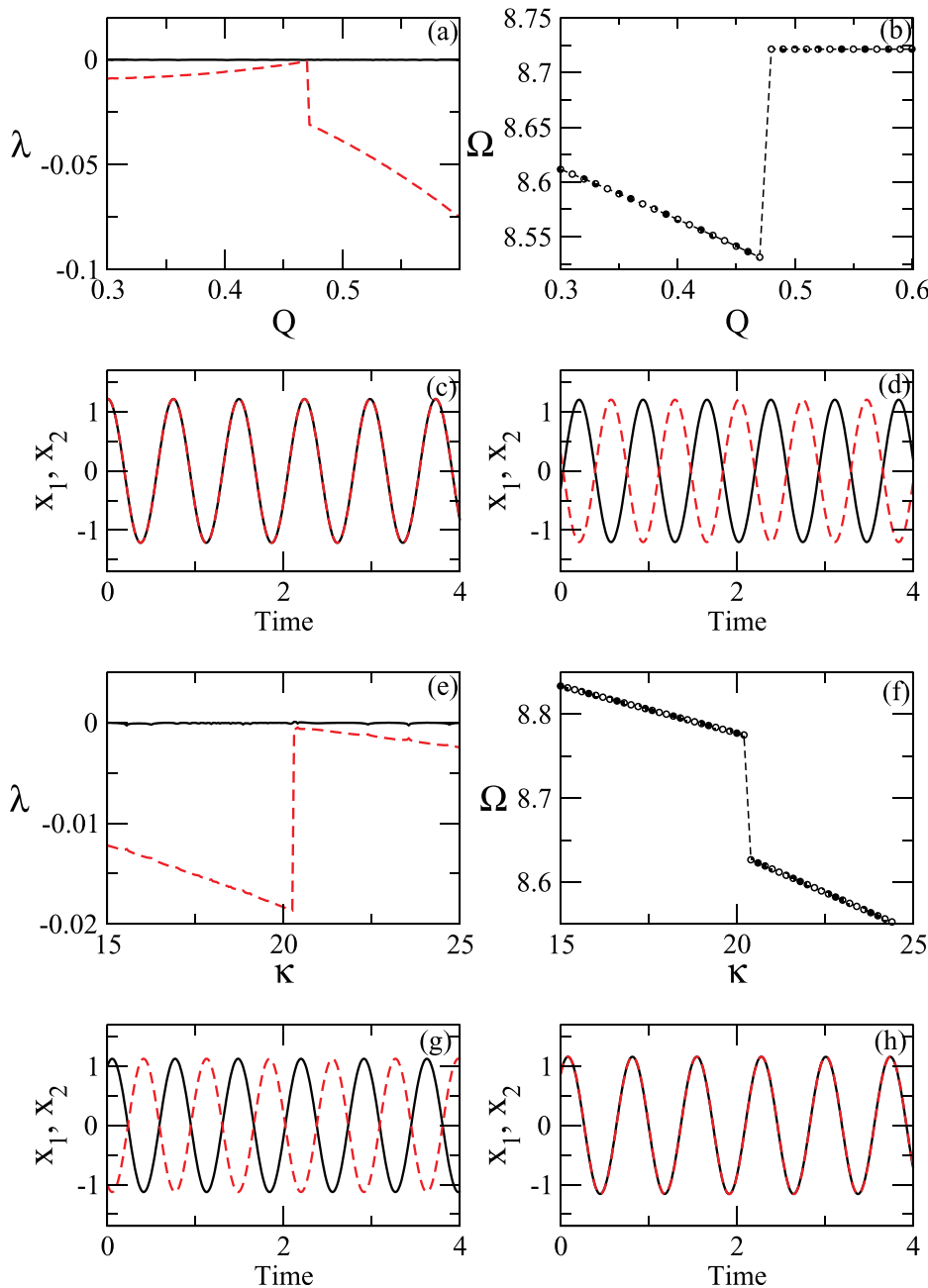


FIG. 3. (a) Spectrum of Lyapunov exponents as a function of environment coupling Q at fixed $\kappa = 25$ and $k_1 = 0.5$. (b) Numerically calculated common frequency Ω of the coupled Landau-Stuart oscillators. (c) In-phase and (d) out-of-phase dynamics before and after the transition at $Q=0.4$ and $Q=0.5$. The largest two Lyapunov exponents (e) and common frequency of coupled systems (f) as a function of κ at $Q = 0.45$ and $k_1 = 0.5$. (g) out-of-phase and (h) in-phase dynamics of coupled system at $\kappa = 18$ and $\kappa = 22$, respectively, before and after $\kappa_c = 20.3$.

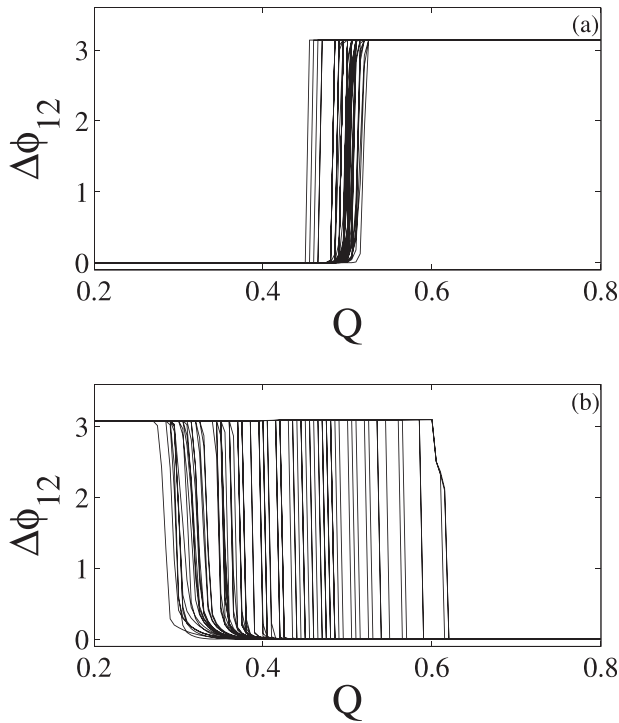


FIG. 4. Bistability in dynamical systems coupled through dynamic environment: phase difference average over time of coupled dynamical system with Q for 100 different initial conditions. (a) Landau-Stuart oscillators at $\kappa = 30$ and (b) *Rössler* oscillators at $\kappa = 20$.

In the white region of the phase diagram (Fig. 5), both systems drive each other to an unbound state. The largest four Lyapunov exponents are plotted in Fig. 6(a). As we increase Q from zero, the first two largest Lyapunov exponent (black and red) become zero while third largest Lyapunov exponent (green) becomes negative that indicates onset of anti-phase synchronization. On further increasing Q , we find a *PF* transition at $Q_c = 0.29$ when the second Lyapunov moves to a negative value accompanied by sharp discontinuities in both the third and the fourth Lyapunov exponents from anti-phase to in-phase in periodic regime. The transition between different dynamical regimes on the *PF* boundary has been studied in detail for delay coupled *Rössler* oscillators.¹⁵ The common oscillation frequency here shows an abrupt change in frequency from 1.03 to 1.07 at $Q_c = 0.29$ in

Fig. 6(b). Time series of the two oscillators show anti-phase synchronization at $Q < Q_c$ in Fig. 6(c) while in-phase synchronization after the transition at $Q > Q_c$ in Figs. 6(c) and 6(d). We also plotted the largest four Lyapunov exponents and common frequency of coupled *Rössler* oscillators by varying κ at $Q = 0.3$ with fixed $k_1 = 0.5$. With an increase of κ from zero, the largest Lyapunov exponents start decreasing. For small κ values, the coupled systems show coexisting states of synchronization and phase difference $\Delta\phi_{12}$ is fluctuating between 0 and π . By further increasing κ , a transition of the first and second Lyapunov from positive to zero shows the anti-phase synchronization in a periodic region at $\kappa = 6.1$. Increasing κ further, we observed transition, in the anti-phase regime, from a periodic to a chaotic regime at $\kappa = 9.2$ and then a second transition to a periodic regime is noted at $\kappa = 15.6$ with zero largest Lyapunov exponents. During these transitions, no *PF* transition is observed. Finally, an abrupt change from zero to negative in second, third, and fourth Lyapunov exponents and in the common frequency of the coupled *Rössler* oscillators is observed at $\kappa_c = 24.6$ that indicates a *PF* transition as shown in Figs. 6(e) and 6(f). A pair of time series of the coupled *Rössler* systems before and after the transition at κ_c is shown in Figs. 6(g) and 6(h). A bistability in phase-flip transition is also found in coupled *Rössler* oscillator and it is again tested by taking 100 different set of initial conditions with Q . The region of bistability, however, is wider compared to the LS system, which fluctuates from 0.29 to 0.63 (see Fig. 4(b)).

IV. EXPERIMENT: COUPLED VAN DER POL OSCILLATORS

In this section, we demonstrated the *PF* phenomenon using electronic circuit of the van der Pol oscillator. For this purpose, we specially designed the environmental coupling in circuit. Consider the following van der Pol oscillator³² with the proposed scheme of environmental coupling

$$\begin{aligned} \dot{x}_i &= y_i, \\ \dot{y}_i &= b(1 - x_i^2)y_i - x_i + \kappa s_i, \\ \dot{s}_i &= -k_0 s_i + k_1 y_i - \eta \left(s_i - \frac{Q}{2} \sum_{j=1}^2 s_j \right), \end{aligned} \tag{10}$$

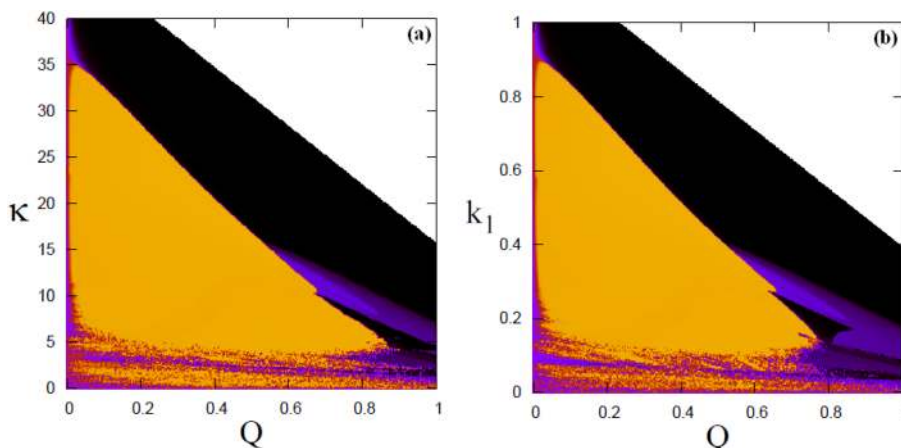


FIG. 5. Phase difference between two *Rössler* oscillators in parameter space (a) $\kappa - Q$ at fixed $k_1 = 0.5$ and (b) $k_1 - Q$ at fixed $\kappa = 20$. Black region shows the in-phase state while yellow out-of-phase state, and white for unbound state.

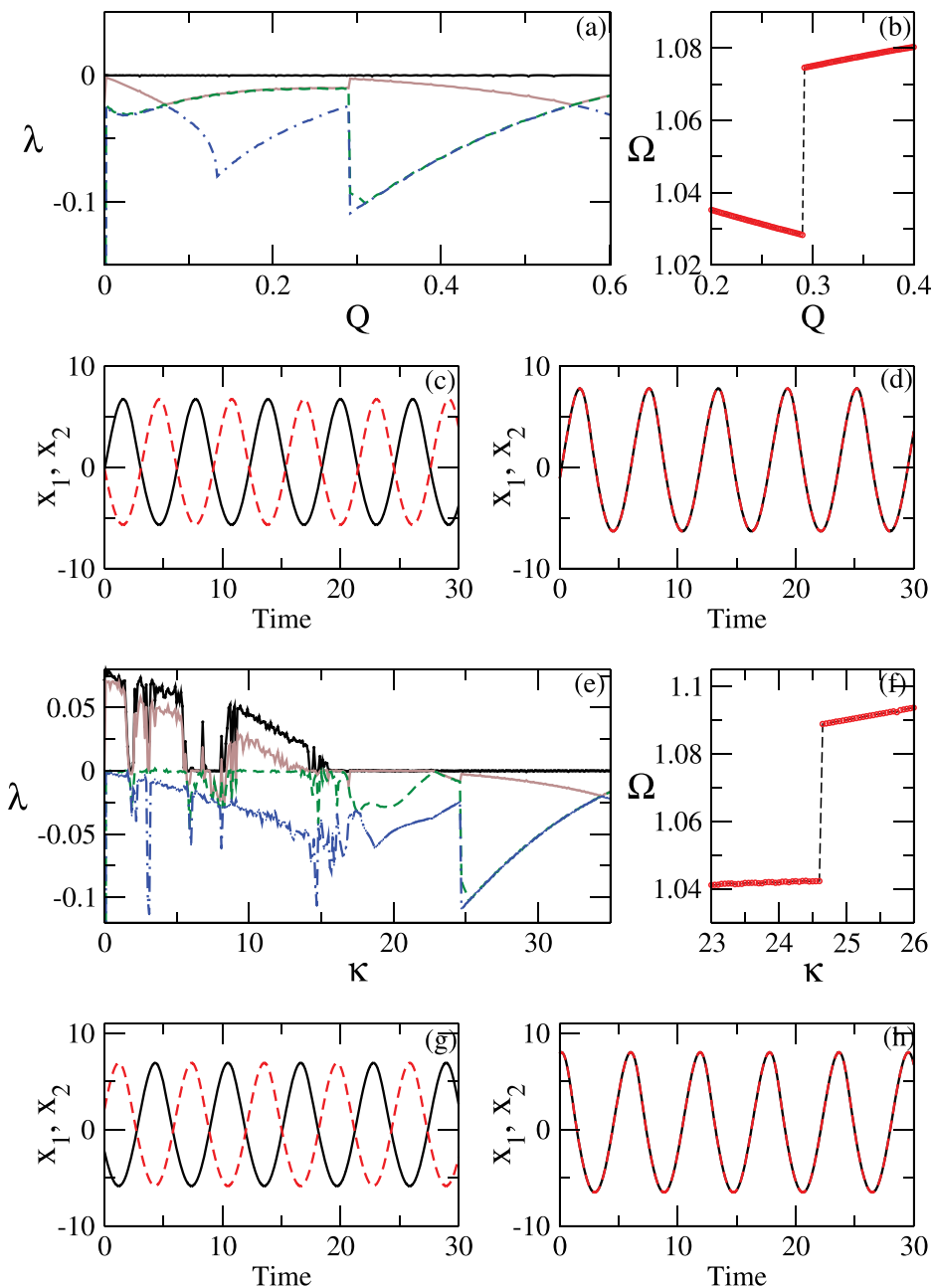


FIG. 6. (a) Spectrum of Lyapunov exponents as a function of environment coupling Q at fixed $k_1 = 0.5$ and $\kappa = 25$. (b) Numerically calculated common frequency Ω of the coupled Rössler oscillators. (c) Anti-phase and (d) in-phase dynamics before and after the transition at $Q = 0.25$ and $Q = 0.35$. The largest two Lyapunov exponents (e) and common frequency of coupled systems (f) as function of κ at fixed parameters $Q = 0.3$ and $k_1 = 0.5$. (g) Out-of-phase and (h) in-phase dynamics of coupled system at $\kappa = 23$ and $\kappa = 26$, respectively, before and after the $\kappa_c = 24.6$.

where the parameters are $b = 1, k_0 = 1, \eta = 1, k_1 = 0.25$. We first use numerical methods to calculate the relative phase difference of coupled van der Pol oscillators in parameter plane $(\kappa - Q)$ by fixing parameter $k_1 = 0.25$. With increasing environment coupling Q , there is a transition from in-phase to anti-phase state shown in Fig. 7. To explore the phase-flip transition, we plot the Lyapunov exponents and common frequency of the coupled van der Pol oscillator with environment coupling Q at $\kappa = 0.56$. With increasing Q , we observed a discontinuity in the second largest Lyapunov exponent and the common frequency of the coupled van der Pol oscillator at $Q_c = 1.4$ that indicates the phase-flip transition from in-phase to antiphase state (see Figs. 8(a) and 8(b)). A corresponding pair of time series of the coupled van der pol oscillator before and after the transition at Q_c for $\kappa = 0.56$ is shown in Figs. 8(c) and 8(d).

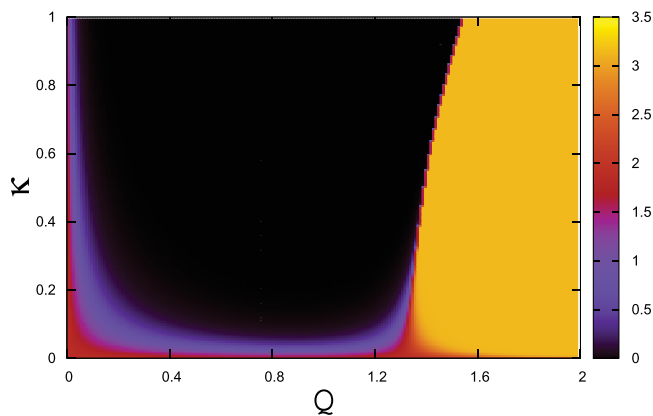


FIG. 7. Phase difference between two van der Pol oscillators coupled through local environment in parameter space $\kappa - Q$ at fixed $k_1 = 0.25$. Black region shows the in-phase state while yellow out-of-phase state.

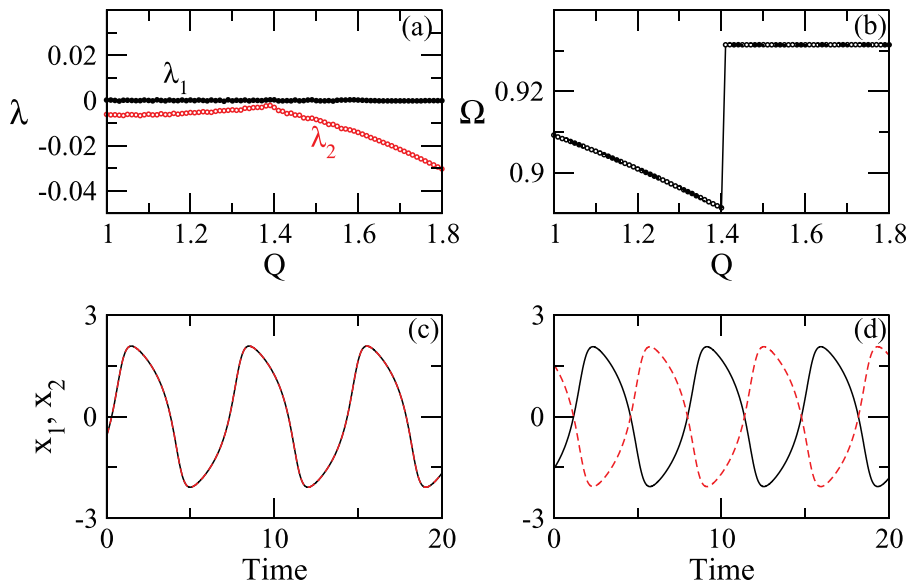


FIG. 8. (a) Spectrum of Lyapunov exponents as a function of environment coupling Q at fixed $k_1 = 0.25$ and $\kappa = 0.56$. (b) Numerically calculated common frequency Ω of the coupled van der Pol oscillators. (c) In-phase and (d) anti-phase dynamics before and after the transition at $Q = 1.2$ and $Q = 1.5$.

Next, we present experimental evidence of the *PF* transition in environmentally coupled oscillators. Electronic circuits of two van der Pol oscillators are constructed as shown in Fig. 9 using six integrators ($U_1 - U_3$ and $U_5 - U_7$) and four multipliers ($A1-A4$: AD633) and, associated resistances and capacitors. Another two integrators (U_8) and (U_{11}) separately represent the dynamics of the two agents of the two oscillators which maintain individual coupling with their respective agents by using (U_{10}) and (U_{12}). The coupling between the two agents is established by using (U_{13}) which

acts as a summing amplifier for the outputs of the agents or the environment circuits $S_{1,2}$. The output of the summing amplifier (SS) is connected to the inputs of the integrators U_8 and U_{11} which produces the mean field effect in the dynamic environment. After the coupling is established, we fixed the parameter $k_1 = \frac{1}{R_{15}} = \frac{1}{R_{21}}$, $\kappa = \frac{1}{R_{14}} = \frac{1}{R_{20}}$ by selecting resistance $R_{15} = R_{21} = 100 \text{ k}\Omega$, $R_{14} = R_{20} = 5.6 \text{ k}\Omega$. The decaying rate of the environment circuits is characterized by $k_0 = \frac{1}{R_{16}} = \frac{1}{R_{22}}$ where the resistance values are selected as $R_{16} = R_{22} = 4.7 \text{ k}\Omega$. The environment coupling Q is

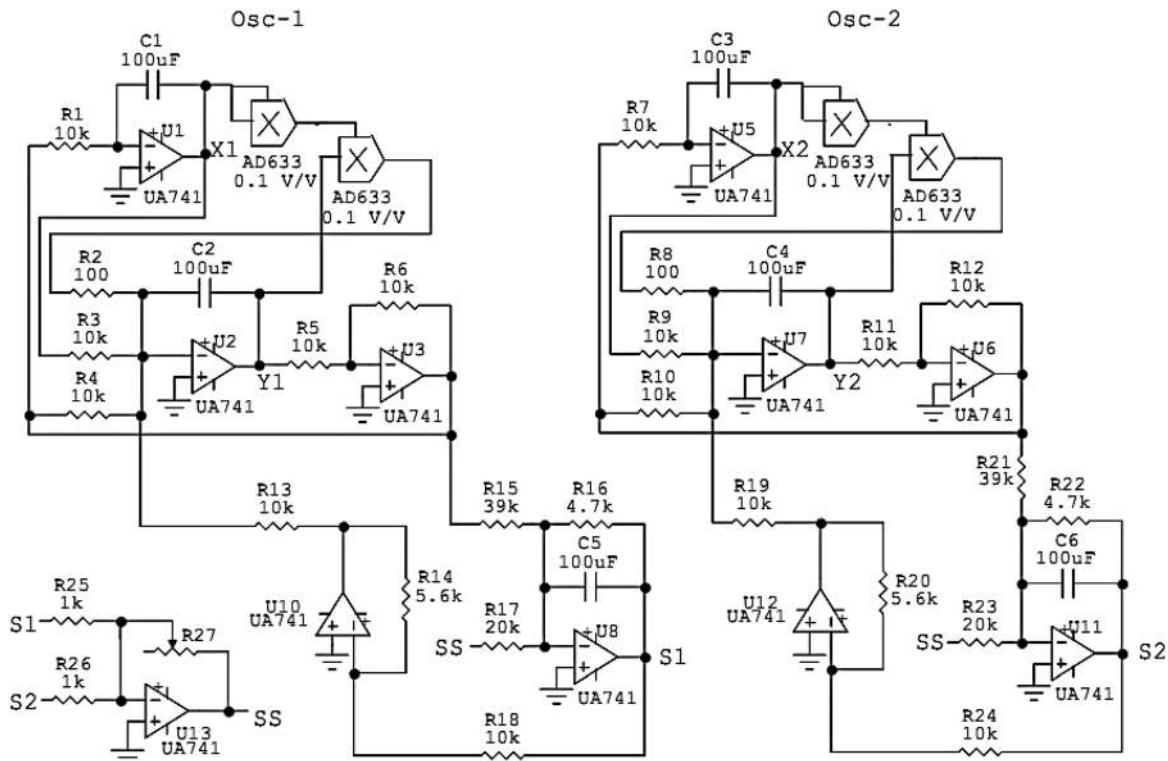


FIG. 9. Circuit of two coupled van der Pol circuit coupled through two local environment circuits. Variable resistance $R = R_{27}$ is used to change the parameter $Q = \frac{R_{25,26}}{R_{27}}$. The circuit is run by $\pm 12 \text{ V}$ power supply.

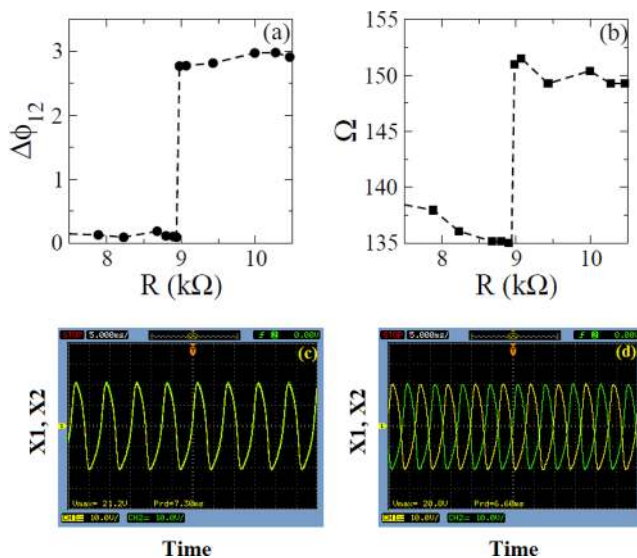


FIG. 10. The average phase difference $\Delta\phi_{12}$ and the common frequency Ω of the coupled van der Pol oscillator through environment circuits as function of variable resistance $R = R_{27}$ shown in (a) and (b). The experimental time series voltage of $X1$ and $X2$ for (b) in-phase dynamics at $R = 8.23$ k Ω and (c) out-of-phase dynamics at $R = 9.9$ k Ω .

controlled by $\frac{R_{27}}{R_{25,26}}$, $R_{25} = R_{26}$ and varied by resistance R_{27} until 15 k Ω . In compliance with the numerical results, for higher Q values, the coupled oscillators are unbounded. Both the van der Pol oscillators and environment circuits are operated by a ± 12 V power supply. The output voltages $X1$ and $X2$ are monitored by using a 2-channel digital oscilloscope (Agilent DSO1012A) with maximum sampling rate 2 GS/s. The instantaneous phase ϕ_i of a measured oscillatory voltage is estimated using Hilbert transform.³³ The frequency of oscillation is estimated by taking an average of rate of change of instantaneous phase. The resulting phase difference $\Delta\phi_{12}$ and common frequency Ω of the coupled van der Pol oscillators are plotted with variable resistance $R = R_{27}$ ($Q = \frac{R_{25,26}}{R_{27}}$) as shown in Figs. 10(a) and 10(b). A sharp jump or discontinuity in phase difference $\Delta\phi_{12}$ and common frequency Ω at $R = 8.94$ k Ω of the coupled oscillator confirms the phase-flip transition. Snapshots of measured time series of $X1$ and $X2$ are shown in Fig. 10. The pair of measured $X1$ and $X2$ time series shows in-phase synchrony for $R = 8.23$ k Ω in Fig. 10(c) while the same pair is in out-of-phase in Fig. 10(d) for resistance $R = 9.99$ k Ω . The experimental results are in close agreement with the numerical results.

V. CONCLUSION

We explored in-phase and anti-phase synchronization and related phase-flip transitions in nonlinear dynamical systems, in general, using a special type of indirect coupling via a common dynamic environment. The *PF* transition is characterized using Lyapunov exponents, oscillation frequency and phase difference as a function of the coupling parameters. Interestingly, we observed the phase-flip transitions in periodic as well as chaotic systems in absence of any delay in the coupling. The *PF* transition is basically induced in the dynamical systems by an indirect interaction via its agents which interact in a common dynamical medium. It appeared

that this particular indirect coupling sets an effective time-delay in transmission of information between the oscillators causing the phase-flip transition similar to what is observed in presence of coupling delay.²⁰ We presented numerical examples of *Landau-Stuart* oscillator and *Rössler* oscillators. We implemented the coupling scheme in an electronic circuit and provided experimental evidence of the phase-flip transition. The transition from in-phase to anti-phase or vice versa depends on the stability of one of the states with a given parameter values or system under study. Also, these are nonlinear systems, which are topologically different from each other, give rise to different range of bistability.

Existences of in-phase and anti-phase were reported earlier^{23,34,35} in cell systems (synthetic genetic networks in *Escherichia coli* cells under inter-cell signaling which is defined here as dynamic environment based coupling). However, a *PF* transition, to our best knowledge, was not reported there. We emphasized, in this report, the existence of in-phase and anti-phase regimes and, the *PF* transition in nonlinear dynamical systems, in general, when coupled through dynamic environment. We thus conclude that a similar phase-flip transition is predictable in other biological systems too, particularly, in synthetic genetic networks²³ and chemical systems.²⁵ The analysis of the phase-flip transition in ensembles of oscillators interacting through a dynamic environment will be of interest, for example, in bacterial quorum sensing, where bacteria releases signaling molecules in the environment which in turn are sensed and used for population coordination. Studies in this direction are currently underway.³⁶

ACKNOWLEDGMENTS

We would like to acknowledge the financial support from DST, India and LNMIIT, Jaipur. A.S. is grateful for the hospitality and facilities provided by the Indian Institute of Chemical Biology (CSIR), Kolkata, during his visit. S.K.D. is supported by the BRNS/DAE, India under Project No. 2009/34/26/BRNS.

- ¹A. Sharma, M. D. Shrimali, A. Prasad, R. Ramaswamy, and U. Feudel, *Phys. Rev. E* **84**, 016226 (2011).
- ²A. S. Pikovsky, M. G. Rosenblum, and J. Kurths, *Synchronization: A Universal Concept in Nonlinear Sciences*, Cambridge Nonlinear Science Series (Cambridge University Press, Cambridge, 2001); references therein.
- ³L. M. Pecora and T. L. Carroll, *Phys. Rev. Lett.* **64**, 821 (1990); H. Fujisaka and T. Yamada, *Prog. Theor. Phys.* **69**, 32 (1983).
- ⁴M. G. Rosenblum, A. S. Pikovsky, and J. Kurths, *Phys. Rev. Lett.* **76**, 1804 (1996); E. R. Rosa, E. Ott, and M. H. Hess, *ibid.* **80**, 1642 (1998).
- ⁵J. Liu, C. Ye, S. Zhang, and W. Song, *Phys. Lett. A* **274**, 27 (2000).
- ⁶S. Sivaprakasam, I. Pierce, P. Rees, P. S. Spencer, K. A. Shore, and A. Valle, *Phys. Rev. A* **64**, 013805 (2001); C. M. Kim, S. Rim, W. H. Kye, J. W. Ryu, and Y. J. Park, *Phys. Lett. A* **320**, 39 (2003); H. Zhu and B. Cui, *Chaos* **17**, 043122 (2007).
- ⁷M. G. Rosenblum, A. S. Pikovsky, and J. Kurths, *Phys. Rev. Lett.* **78**, 4193 (1997).
- ⁸N. F. Rulkov, M. M. Sushchik, L. S. Tsimring, and H. D. I. Abarbanel, *Phys. Rev. E* **51**, 980 (1995); L. Kocarev and U. Parlitz, *Phys. Rev. Lett.* **76**, 1816 (1996).
- ⁹S. Boccaletti and D. L. Valladares, *Phys. Rev. E* **62**, 7497 (2000); M. A. Zaks, E. H. Park, M. G. Rosenblum, and J. Kurths, *Phys. Rev. Lett.* **82**, 4228 (1999).
- ¹⁰I. Grosu, R. Banerjee, P. K. Roy, and S. K. Dana, *Phys. Rev. E* **80**, 016212 (2009); A. Prasad, *Chaos, Solitons Fractals* **43**, 42 (2010); A. Sharma and

- M. D. Shrimali, *Nonlinear Dyn.* **69**, 371 (2012); S. K. Bhowmik, D. Ghosh, and S. K. Dana, *Chaos* **21**, 033118 (2011).
- ¹¹D. G. Aronson, G. B. Ermentrout, and N. Kopell, *Physica D* **41**, 402 (1990).
- ¹²R. Karnatak, R. Ramaswamy, and A. Prasad, *Phys. Rev. E* **76**, 035201 (2007); R. Karnatak, R. Ramaswamy, and A. Prasad, *Chaos* **19**, 033143 (2009).
- ¹³D. V. Raman Reddy, A. Sen, and G. L. Johnston, *Phys. Rev. Lett.* **80**, 5109 (1998).
- ¹⁴A. Prasad, M. Dhamala, B. M. Adhikari, and R. Ramaswamy, *Phys. Rev. E* **81**, 027201 (2010); **82**, 027201 (2010).
- ¹⁵A. Prasad, J. Kurths, S. K. Dana, and R. Ramaswamy, *Phys. Rev. E* **74**, 035204 (2006).
- ¹⁶A. Prasad, *Phys. Rev. E* **72**, 056204 (2005).
- ¹⁷P. R. Sharma, A. Sharma, M. D. Shrimali, and A. Prasad, *Phys. Rev. E* **83**, 067201 (2011).
- ¹⁸M. Y. Kim, R. Roy, J. L. Aron, T. W. Carr, and I. B. Schwartz, *Phys. Rev. Lett.* **94**, 088101 (2005).
- ¹⁹J. M. Cruz, J. Escalona, P. Parmananda, R. Karanatak, A. Prasad, and R. Ramaswamy, *Phys. Rev. E* **81**, 046213 (2010).
- ²⁰A. Prasad, S. K. Dana, R. Karnatak, J. Kurths, B. Blasius, and R. Ramaswamy, *Chaos* **18**, 023111 (2008).
- ²¹B. M. Adhikari, A. Prasad, and M. Dhamala, *Chaos* **21**, 023116 (2011).
- ²²D. McMillen, N. Kopell, J. Hasty, and J. J. Collins, *Proc. Natl. Acad. Sci. U.S.A.* **99**, 679 (2002).
- ²³E. Ullner, A. Zaikin, E. Volkov, and J. G. Ojalvo, *Phys. Rev. Lett.* **99**, 148103 (2007); E. Ullner, A. Koseska, J. Kurths, E. Volkov, H. Kantz, and J. G. Ojalvo, *Phys. Rev. E* **78**, 031904 (2008).
- ²⁴M. Bennett, M. F. Schatz, H. Rockwood, and K. Wiesenfeld, *Proc. R. Soc. London, Ser. A* **458**, 563 (2002).
- ²⁵A. F. Taylor, M. R. Tinsley, F. Wang, Z. Huang, and K. Showalter, *Science* **323**, 614 (2009).
- ²⁶D. Gonze, S. Bernard, C. Waltermann, A. Kramer, and H. Herzel, *Bio-phys. J.* **89**, 120 (2005).
- ²⁷J. Javaloyes, M. Perrin, and A. Politi, *Phys. Rev. E* **78**, 011108 (2008).
- ²⁸C. L. Tang, H. Statz, and G. deMars, *J. Appl. Phys.* **34**, 2289 (1963); K. Wiesenfeld, C. Bracikowski, G. James, and R. Roy, *Phys. Rev. Lett.* **65**, 1749 (1990).
- ²⁹G. Katriel, *Physica D* **237**, 2933 (2008); V. Resmi, G. Ambika, and R. E. Amritkar, *Phys. Rev. E* **81**, 046216 (2010); **84**, 046212 (2011); A. Sharma and M. D. Shrimali, *Pramana, J. Phys.* **77**, 881 (2011).
- ³⁰R. Karnatak, N. Punetha, A. Prasad, and R. Ramaswamy, *Phys. Rev. E* **82**, 046219 (2010).
- ³¹O. Rössler, *Phys. Lett.* **57A**, 397 (1976).
- ³²B. van der Pol and J. Van der Mark, *Nature* **120**, 363 (1927).
- ³³D. Gabor, *J. Inst. Electr. Eng., Part 3* **93**, 429 (1946).
- ³⁴J. Garcia-Ojalvo, M. B. Elowitz, and S. H. Strogatz, *Proc. Natl. Acad. Sci. U.S.A.* **101**, 10955 (2004).
- ³⁵M. R. Bennett and J. Hasty, *Nat. Genet.* **39**, 146 (2007).
- ³⁶A. Sharma *et al.* (unpublished).